ACS SENSORS

pubs.acs.org/acssensors

Article

Solid-State Nanopore Sizing for cfDNA Sample Quality Control in Point-of-Need Sequencing

Muhammad Asad Ullah Khalid, Md. Ahasan Ahamed, Anthony J. Politza, and Weihua Guan*

Cite This: *ACS Sens.* 2025, 10, 5674−5683

Read Online

ACCESS | Metrics & More | Article Recommendations | Supporting Information

Downloaded via INDIANA UNIV BLOOMINGTON on September 3, 2025 at 18:32:08 (UTC).
See https://pubs.acs.org/sharingguidelines for options on how to legitimately share published articles.

ABSTRACT: DNA sequencing is a powerful tool for diagnosing conditions such as infectious diseases and cancers. Even though current workflows demand rigorous quality control (QC) of DNA samples, this QC is typically limited to lab settings despite recent advances in portable nanopore sequencers. For personalized health care to truly benefit from the portable sequencer, QC must be performed right where the samples are processed. Here, we present a solid-state nanopore device that provides label-free, controlled quantification and qualification of cell-free DNA (cfDNA). We demonstrated the use of a 1 kbp double-stranded DNA internal marker at a known concentration to measure the concentration of a representative cfDNA target in the presence of genomic DNA. We also found that nanopores with diameters ranging from 6 to 19 nm yield consistent measurements with a maximum coefficient of variation (CV) of less than 15%. Moreover, analyzing data from multiple nanopores over longer acquisition times can reduce the uncertainty to below 10% CV. Finally, we applied our nanopore QC assay to a plasma cfDNA sample and compared the results to those from a capillary electrophoresis (CE) assay. Both methods produced highly correlated measurements, demonstrating the potential of our nanopore QC assay for effective cfDNA assessment at the point of need.

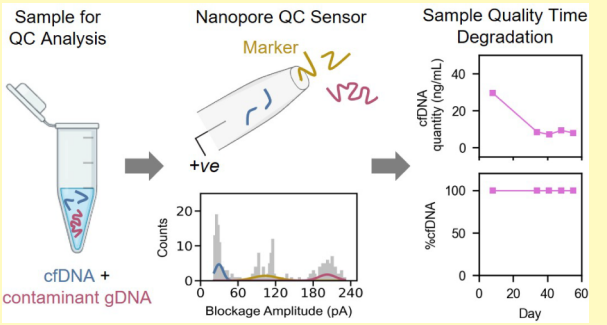

KEYWORDS: *cell-free DNA, plasma, quality control, nanopore, sequencing, point-of-need*

Advancements in DNA sequencing technologies have revolutionized clinical diagnostic and therapeutic practices.[1−4] However, traditional sequencing platforms such as Sanger Sequencing,[5] Illumina Sequencing—Sequence By Synthesis (SBS),[6,7] Sequence By Ligation (SBL),[8] and PacBio Single Molecule Real-Time (SMRT) sequencing,[9] etc. remain confined to centralized laboratories due to their size, cost, and infrastructure requirements. Point-of-need sequencing can address these challenges by bringing sequencing capabilities directly to the sample collection site, offering rapid, portable, and decentralized analysis. It can also enable personalized and faster clinical decision-making,[10] rapid real-time genomic surveillance of infectious outbreaks,[11,12] and field-based environmental and agricultural monitoring.[13] Portable sequencers such as MinION from Oxford Nanopore Technologies (ONT) have demonstrated high potential for enabling (PoN) sequencing to accelerate the developments in personalized medicine for DNA-based diagnostics.[14−16] However, genomic sequencing is a multistep process that includes sample collection, sample quality control, and library preparation before subjecting it to actual downstream sequencing analysis.[17] Although the portability of MinION makes it suitable for PoN applications, sample quality control remains the bottleneck for the true implementation of point-of-need sequencing workflows.

For instance, the quality of the cfDNA sample is a critical determinant in sequencing outcomes and should be rigorously assessed before proceeding with downstream library preparation and sequencing workflows. Typically, a larger quantity of total cfDNA and higher relative abundance of mononucleosomes in cfDNA samples is ideal for NGS[18] mutation analysis toward cancer detection, treatment monitoring, and detection of relapses. On the contrary, a higher relative abundance of larger sizes (di- and tri-nucleosomes) can lead to issues during library preparation steps, potentially causing incomplete adapter ligation or biased amplification.[19] This can reduce sequencing efficiency and read quality, which also suggests the determination of both total cfDNA concentration and % cfDNA before library preparation for the sequencing workflow. Additionally, the cfDNA sample can most often be contaminated with high molecular weight (HMW) genomic (g) DNA, from the lysis of leukocytes, released in plasma during sample preparation,[20,21] leading to decreased sensitivity

Received: March 10, 2025
Revised: June 10, 2025
Accepted: June 20, 2025
Published: June 26, 2025

ACS Publications

© 2025 American Chemical Society

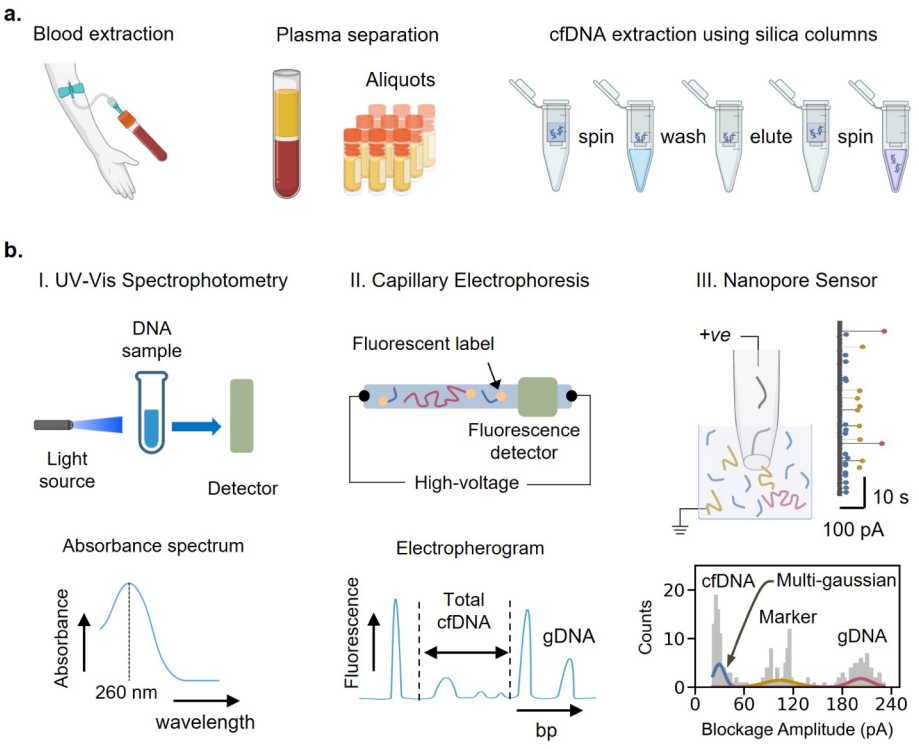

c.

	UV-Vis Spectrophotometry	Capillary Electrophoresis	Nanopore Sensor
cfDNA concentration	NO	YES	YES
%cfDNA	NO	YES	YES
Total DNA	YES	YES	YES
Detection method	Label-free	Fluorescent labels	Label-free
POC ammendability	NO	NO	YES

Figure 1. Scheme for cfDNA sample quality control using conventional strategies and proposed nanopore sensing: (a) Blood collection for plasma separation by double centrifugation with aliquot preparation, followed by cfDNA extraction using silica-based membrane columns according to manufacturer's protocol before subjecting to quality control procedures. (b) Conventional cfDNA quality control procedures include the following: (I) UV−vis spectrophotometric absorbance at 260 nm, which only provides total DNA concentration, and (II) capillary electrophoresis, which can provide total DNA quantity, total cfDNA quantity, and %cfDNA but requires fluorescent labels, detector, and high voltage operation. (III) However, our proposed label-free glass nanopore sensor scheme performs quantification of extracted total cfDNA as well as %cfDNA from the complex DNA samples containing 1 kbp DNA marker. This is accomplished by processing ionic current—time data for single molecule analysis of the complex DNA sample using blockage amplitude distribution and multi-Gaussian fitting to extract individual frequencies f_T, f_M, and f_{gDNA} of the component cfDNA, marker, and HMW gDNA fragments. The frequencies are then used for the estimation of total cfDNA concentration and the determination of %cfDNA. (c) A multiparametric comparison of different quality control techniques.

or inconsistent results in NGS assays.[22] Similarly, the presence of organic contaminants from extraction processes can easily incur under- or overestimation of the cfDNA spectrophotometric concentrations.[23,24] Therefore, tight quality control (QC) steps are required to ensure that extracted cfDNA samples are the right fit for downstream sequencing workflows. Traditionally, the nanodrop spectrophotometer is used to quantify total DNA with a limit of detection (LOD) as low as <1 ng/μL; however, it cannot provide information on the fragment length or the DNA integrity of the sample,[25,26] which is not desirable for cfDNA sample QC. Similarly, Qubit fluorometric assays can quantify total dsDNA, ssDNA, or RNA samples but are unable to provide fragmentation information on DNA.[27] To quantify and assess the fragment size profiles of cfDNA samples, capillary electrophoresis (CE) is often employed. It performs electrophoretic separation of cfDNA fragments, often categorized as mononucleosome (~165 bp), dinucleosome (~350 bp), and trinucleosome (~565 bp) fragments[28] because of their apoptotic or necrotic origin, in addition to the HMW gDNA (~ 10 kbp or more). However, a typical CE process requires the use of fluorescent dyes with large input sample quantities, complex instrumentation to perform high-voltage electrophoresis, fluorescence/UV detectors, and trained personnel to operate.[29] Conversely, PCR-based approaches focus on the amplification of specific gene fragments only,[24,30] which limits their use cases for quantification of total cfDNA—essential for sample QC before sequencing. Collectively, these approaches are also tedious, time-consuming, and not amendable for field applications. To enable true point-of-need DNA sequencing applications, there is a critical need for a point-of-need amendable sample quality assessment tool.

In this work, we developed a nanopore sensor aimed at performing amplification-free and label-free quality assessment of plasma cfDNA samples that can be amendable for point-of-need applications. Our proposed technique utilizes marker

https://doi.org/10.1021/acssensors.5c00803
ACS Sens. 2025, 10, 5674−5683

DNA as an internal control to perform cfDNA quantification based on size profiling using count distributions of blockage amplitudes. The multi-Gaussian fitting of these blockage amplitude distributions allows the computation of individual event frequencies for the translocation of variably sized DNA components. Subsequently, the event frequencies for the target cfDNA and marker DNA molecules (at a known concentration) are then used to estimate the cfDNA concentration. Since the extracted cfDNA samples may contain a fraction of known characteristic HMW gDNA contaminants, our proposed method also enables the relative quantification of total cfDNA (or %cfDNA) as a qualitative metric. We first demonstrated the precise quantification and qualification of 150 bp model DNA fragments as a representative cfDNA target using a 1 kbp DNA marker in mock samples also containing 10 kbp as a representative HMW gDNA at known concentrations. We then analyzed the uncertainty in our nanopore measurements by processing the cumulative data from one, two, three, and four nanopores with data acquisition times from 5 to 30 min for a single mock sample with fixed concentrations of individual model fragments. Our findings revealed that the measurement uncertainty decreased with longer data acquisition times but increased with the number of nanopores used. We further evaluated the applicability of the nanopore QC assay by analyzing the aging of a commercially purchased plasma sample from a healthy individual. Both the nanopore QC assay and a traditional capillary electrophoresis assay showed similar degradation trends in measured cfDNA concentration, with no effect on %cfDNA. The comparison between our nanopore QC assay and the capillary electrophoresis assay indicated negligible differences in individual measurements of cfDNA concentration and %cfDNA. These results suggest that the nanopore QC assay is a robust and comprehensive tool for cfDNA sample quality assessment.

RESULTS AND DISCUSSION

cfDNA Sample Quality Control Using Nanopore Size Counting. To assess the quality of cfDNA in complex human plasma or serum samples, a typical sample preparation workflow is shown schematically in Figure 1a, where blood is collected from healthy or diseased individuals in EDTA collection tubes, followed by a two-step centrifugation at 2000 × g at 4 °C for 10 min for plasma separation and aliquot preparation.[20,31] These plasma samples are then used for cfDNA extraction using, for example, commercially available silica-based membrane columns[32] according to the manufacturer's protocol. Before any downstream analysis, these extracted samples are subjected to Agilent Tapestation 4150 or Bioanalyzer 2100 (for CE), Nanodrop spectrophotometer (Thermo Fisher Scientific, Waltham, MA), or Qubit fluorometer (Invitrogen, Life Technologies) for size profiling and quantitative analysis, respectively.[24] We present here a glass nanopore sensor for the comprehensive quality assessment of these extracted cfDNA samples, as shown in Figure 1b, due to its ability to perform label-free size counting of short fragments. The extracted cfDNA samples are diluted with a 1 kbp dsDNA marker having a 100 pM final concentration in a 4 M LiCl Tris-EDTA (pH 8.0) buffer as an internal control. The use of high salt concentration as a nanopore measurement buffer can be signified by its detection capability of short DNA fragments[33] without any requirements of labels, nanopore surface modifications, or the use of hydrogels as entropic barriers to slow down DNA translocations. An ∼10 nm nanopore diameter, fabricated using a laser puller filled with the salt solution, is inserted into the complex DNA sample containing cfDNA. A positive bias is applied to the patch electrode for ionic current data recording. By analyzing ∼25 − 30 min *I-t* trace data from the nanopore using a custom MATLAB script, the event scatter is plotted to obtain count distributions of blockage amplitudes. A multi-Gaussian fit to the blockage amplitude distributions allows for the computation of individual event frequencies for the translocations of cfDNA targets, marker (M) DNA (1 kbp), and HMW gDNA. To measure the total concentration of cfDNA, an internal calibrator-assisted concentration measurement approach is adapted from Charron et al.[34] The precisely known concentration of our internal 1 kbp marker (C_M) along with cfDNA target and marker frequencies (f_T and f_M) are used to mathematically estimate the total cfDNA concentration (C_T) using $C_T = C_M \times \frac{f_T}{f_M}$ relation valid for diffusion-limited transport. Similarly, the cfDNA target frequency (f_T) and the HMW gDNA frequency (f_{gDNA}) values are used for % cfDNA measurement using $\%\text{cfDNA} = \frac{f_T}{f_T + f_{gDNA}} \times 100$. The frequency values are used here instead of total counts to compensate for data loss due to possible timed clogging of the nanopores during the experiments. The estimated C_T and % cfDNA values are then used as QC metrics of cfDNA for decision-making toward NGS library preparation. A multiparametric comparison of the proposed technology with standard laboratory procedures is presented in Figure 1c. Although this nanopore-based sample QC strategy is demonstrated for cfDNA (∼165 bp) quantification and qualification, it can be adopted for DNA targets of different lengths. To design the nanopore-based sample QC for DNA targets of lengths other than cfDNA, various optimizations will include careful selection of marker DNA, workable range of nanopore diameter, and strength and types of salt buffers.

Quantification and Qualification of 150 Bp dsDNA from the Mock Samples Using Nanopore Sensor. To enable the quantification of cfDNA in the plasma samples using nanopore sensor, we first evaluated the ability of our nanopore sensor to quantify 150 bp dsDNA as a representative cfDNA target (T) in a mock sample with 10 kbp dsDNA as a high molecular weight (HMW) gDNA contaminant and 1 kbp dsDNA as an internal marker (M) in 4 M LiCl Tris-EDTA (pH 8.0) measurement buffer. The 1 kbp marker positions itself at an optimal position on the DNA length scale for reliable quantification and qualification of 150 bp (representative cfDNA) in complex samples, which may contain HMW gDNA (≥10 kbp). The marker length is not too close to the cfDNA target length to avoid Gaussian signal overlaps with possible di- and trinucleosomes due to poor size resolution of bare glass nanopores. It is also not too far on the length scale for the same signal overlap issues that may arise from the individual large-variance Gaussians of HMW contaminant DNA. Seven different mock samples were prepared by varying the concentration of the 150 bp target in the range of 10−200 pM and keeping the concentrations of marker and HMW DNA constant at 100 pM each. Test concentrations ranging from 10 to 200 pM were selected to represent the expected cfDNA yield (2−40 ng/mL) in plasma. These values correspond to cfDNA (150 bp target in this case) eluted in 50 μL elution buffer and subsequently diluted 40-fold in 4 M LiCl measurement buffer. All the mock samples were tested using glass

https://doi.org/10.1021/acssensors.5c00803
ACS Sens. 2025, 10, 5674−5683

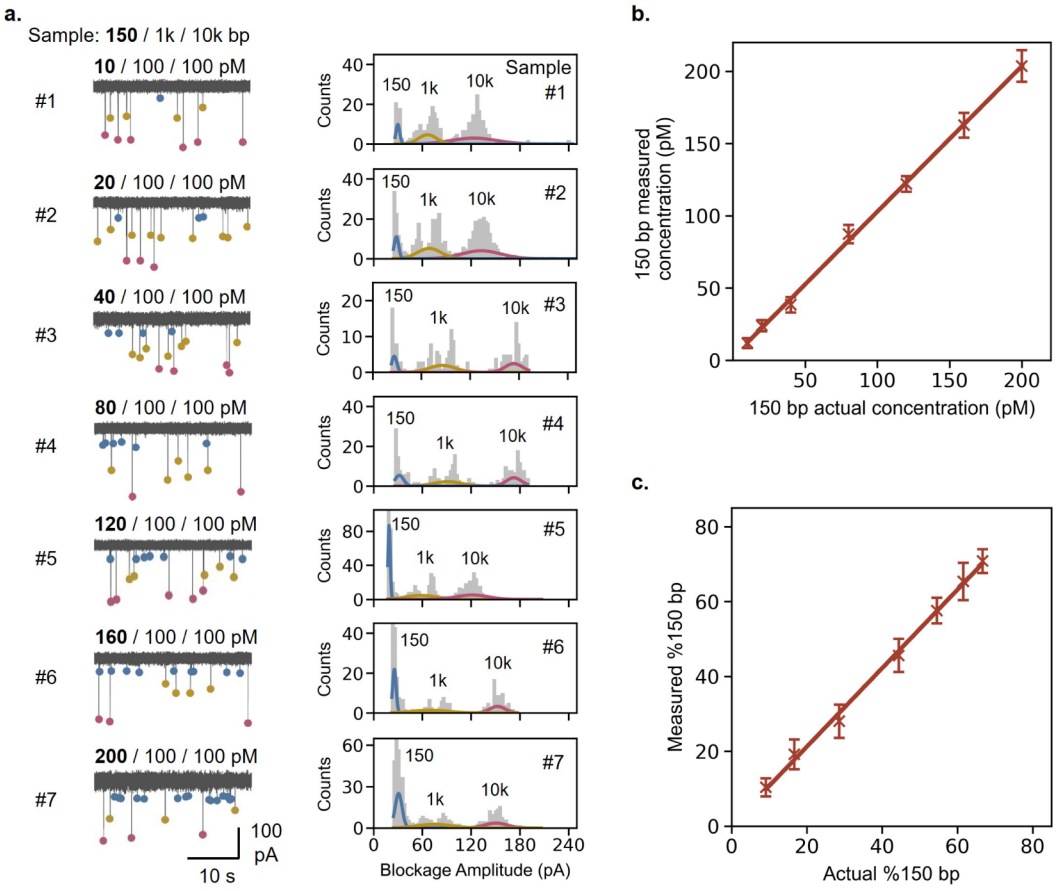

Figure 2. Nanopore sensor-based quantification and qualification of 150 bp dsDNA from different mock samples. (a) Representative *I-t* traces and count histograms of the mock samples with variable concentrations (10−200 pM) of 150 bp dsDNA, where concentrations of 1 kbp marker (M) dsDNA and 10 kbp dsDNA (HMW) were fixed at 100 pM each. Correlation of measured vs actual (b) concentration (pM) and (c) % of 150 bp dsDNA. Data have been presented as $\mu \pm \sigma$ (n = 3).

nanopore devices fabricated using a laser pipette puller with diameters between ∼8 and 18 nm. The ionic current−time (*I-t*) data were recorded at 100 kHz sampling frequency and 5 kHz filter for all the mock samples using Axon Axopatch 200B amplifier for 30 min each as a single measurement. The current blockage event data were then extracted using a custom MATLAB script for each mock sample. These data were further processed in a custom python program to plot count distributions of blockage amplitudes with multi-Gaussian fitting using a Gaussian Mixture Model (GMM). The total individual counts under each Gaussian were then used to determine the individual event frequencies of 150 bp, 1k bp, and 10k bp dsDNA targets and hence the concentration and percentage of 150 bp dsDNA, as previously discussed. In Figure 2a, the representative *I-t* traces of seven different mock samples have been shown. These *I-t* traces implicitly show the increasing frequency of the translocation events for 150 bp dsDNA, as indicated by blue circles in a concentration-dependent manner. This was further confirmed by the associated multi-Gaussian fittings of the count distributions of blockage amplitudes for all seven mock samples, as shown in Figure 2a, where the relative counts for 150 bp dsDNA translocations were increasing. The Gaussian distributions for 1k and 10k bp dsDNA show successively decreasing relative counts distributions despite their fixed concentrations in the mock samples. This is understandable because the capture in diffusion limited transport is DNA length independent while simultaneously being concentration dependent.[34] The transport in our nanopore sensor is diffusion limited because we have utilized bare glass nanopores with sizes varying from >5 nm to <20 nm with high concentration —4 M LiCl symmetric salt eliminating the possibility of encountering an energy barrier due to surface, charges, steric effects, or entropic barriers. The Deby length - λ_D (in water at room temperature) can be calculated from $\lambda_D = \sqrt{\frac{\varepsilon_r \varepsilon_0 k_B T}{2 N_A e^2 I}} = \frac{0.304}{\sqrt{c(M)}}$ for 4 M LiCl salt, where ε_r, ε_0, k_B, T, N_A, e, I, and $c(M)$ represent the relative permittivity, permittivity of free space, Boltzmann's constant, temperature, Avogadro's constant, elementary charge, ionic strength, and molar concentration of the salt solution, respectively.[35] λ_D is found to be ∼0.15 nm,[36] which is much smaller than the nanopore diameters used. This short λ_D (∼0.15 nm) implies that an ∼2 nm wide dsDNA molecule does not feel any electrostatic repulsion or barrier effects from the surface of the glass nanopore when it reaches the entrance to translocate. Additionally, a nanopore diameter range of 5−20 nm is much larger than the dsDNA diameter (∼2.2 nm), which indicates the presence of negligible or minor entropic barriers (even though ∼10 kbp longer HMW gDNA may coil slightly). This analysis validated that our nanopore-based cfDNA quantification and qualification tool followed a diffusion-limited transport model. An above 99% correlation between measured and actual concentrations and the percentage of 150 bp dsDNA, as shown in Figure 2b,c,

https://doi.org/10.1021/acssensors.5c00803
ACS Sens. 2025, 10, 5674−5683

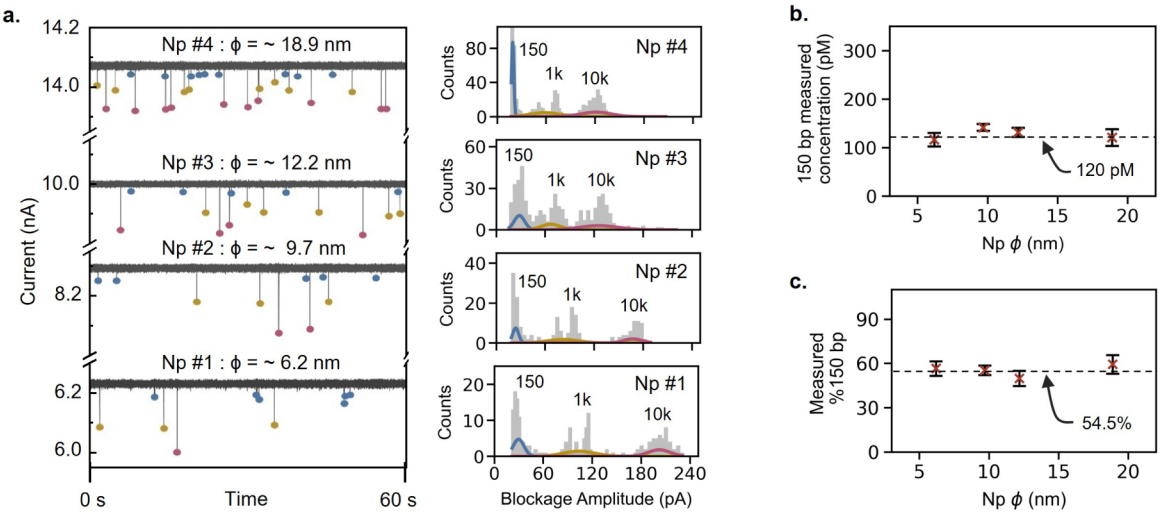

Figure 3. Quantification and qualification of 150 bp dsDNA from a fixed mock sample using different nanopore sensors. (a) Representative *I-t* traces and count histograms for the mock sample 150/1k/10k bp (at 120/100/100 pM) obtained using different nanopores with diameters in the range of 6−19 nm. (b) Measured concentration of 150 bp and (c) measured %150 bp vs Np ϕ (nm). Data have been presented as $\mu \pm \sigma$ (n = 3).

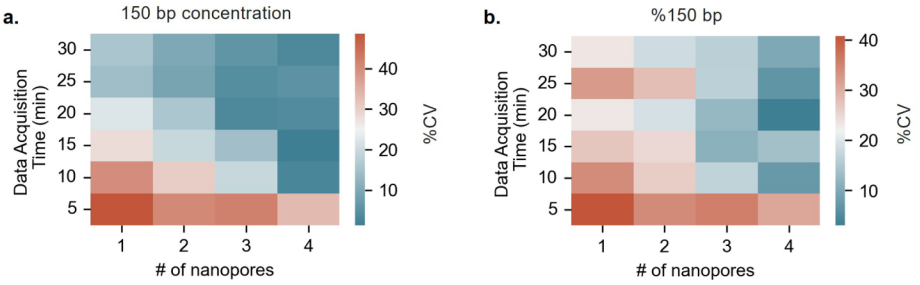

Figure 4. Utilizing data from multiple nanopores to potentially reduce the measurement error and turnaround times of the nanopore QC test. Heatmaps for %CV values of measured (a) 150 bp concentrations and (b) %150 bp from different combinations of data acquisition times and number of nanopores (number of measurements n = 3, $\mu \pm \sigma$).

suggested the highly precise quantification ability of our nanopore sensor in mock samples containing three different targets with length ratios as large as 67×. Although data for the various mock samples were obtained using nanopores with diameters ranging from 8 to 18 nm, a systematic analysis was subsequently conducted to examine the nanopore size-dependent variations in the measurements of concentration and the percentage of 150 bp dsDNA, as discussed below.

To deal with the heterogeneity in nanopore size during measurements, four different glass nanopores were fabricated using laser pipette puller, with respective pore diameters estimated to be ~6.2, 9.7, 12.2, and 18.9 nm. The IV curves and open-pore conductance values used for pore size estimations are provided in Figure S1. Each glass nanopore was tested with mock samples of 150 bp, 1k bp, and 10k bp dsDNA at fixed concentrations of 120, 100, and 100 pM, respectively. The capture rate is expected to increase with the increase in nanopore diameter (from 6.2 to 18.9 nm) and hence the capture radius, which can be seen from the *I-t* traces and multi-Gaussian fittings of the count distributions of blockage amplitudes in Figure 3a. The increase in nanopore diameters can also be confirmed from the shrinkage of blockage distributions for 1k and 10k bp, for Np no. 1 to 4, on the blockage amplitude scales. Interestingly, these populations also imply relatively higher counts for 150 bp dsDNA at 120 pM as compared to 1k and 10k bp at 100 pM each, which is expected. The concentration and percentage of 150 bp dsDNA were estimated using a previously established method and plotted against nanopore diameter (Np ϕ) (data presented as n = 3, $\mu \pm \sigma$), as shown in Figure 3b,c. The dashed lines show the actual concentration of 120 pM and 54.5% of 150 bp dsDNA, respectively. The coefficient of variation (CV) for the measured 150 bp concentrations of Np no. 1−4 were found to be 11.9, 5.1, 7.3, and 14.4%, respectively, suggesting negligible variability between concentration measurements. Similarly, the CV values of 8.6, 5.8, 10.3, and 10.7% for the measured percentage of 150 bp dsDNA also implied insignificant variability in these measurements. The diameter and angle variation in conical nanopores affect the translocation rates of DNA molecules in general.[37] However, the internal marker-based controlled counting approach accommodates such variation by observing proportional changes in the translocation rate of 1 kbp marker DNA. Our analysis suggested that nanopore diameter did not affect the measurements significantly, hence enabling the use of our nanopore sensor for QC of the actual percentage of 150 bp dsDNA from plasma samples. As the analysis time is dependent on the time for data acquisition, we further sought to evaluate the cumulative data from multiple nanopores and for different data acquisition times before conducting validation studies using a plasma cfDNA sample.

https://doi.org/10.1021/acssensors.5c00803
ACS Sens. 2025, 10, 5674−5683

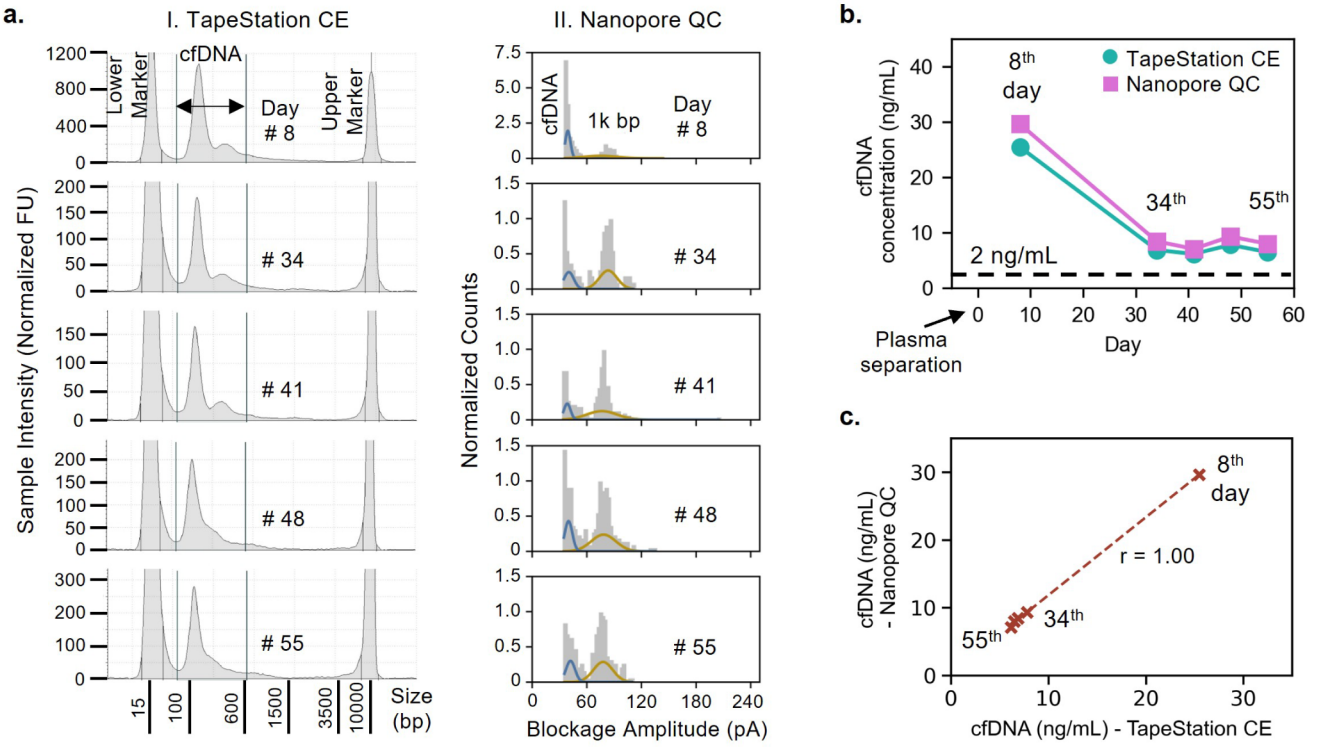

Figure 5. Validation of nanopore QC test using the plasma sample of a healthy individual. (a) Electropherograms obtained from TapeStation capillary electrophoresis (CE) assay with corresponding count distributions of blockage amplitudes from nanopore QC assay. (b) Consistent drop observed in measured cfDNA concentrations using both TapeStation CE and nanopore QC assays at different days up until the 55th day post plasma separation. cfDNA concentration. (c) Measured concentrations of cfDNA using both Nanopore QC and TapeStation CE assays showed high correlation validating the proposed assay's QC performance.

Evaluating Measurement Uncertainty of Nanopore QC Assay. To assess the uncertainty of our nanopore sensor measurements, we analyzed the cumulative data from multiple nanopore configurations with different data acquisition times. The nanopore configurations of one, two, three, and four nanopores were compared against data acquisition times of 5, 10, 15, 20, 25, and 30, each creating a total of 24 test combinations. The mock sample of 150 bp:1k bp:10k bp at fixed concentrations of 120:100:100 pM, respectively, was tested to compute the measurement errors in all 24 test combinations. Four different nanopores were fabricated using a laser pipette puller, with diameters estimated within 9.7 ± 0.8 nm using open-pore conductance data from *I-V* characteristics shown in Figure S2. Each nanopore was used to acquire current−time (*I-t*) data in 5 min chunks for a total of 90 min using an Axopatch 200B amplifier system, which was processed using a custom MATLAB script to obtain blockage amplitudes, as described previously. The processed data were then divided into 24 test combinations, as described above, according to the number of pores and data acquisition times. The measurements of concentration and percentage of 150 bp for each combination were performed according to the internal marker (1 kbp) controlled method described previously. The representative count distributions of blockage amplitudes, along with their respective multi-Gaussian fittings, have been presented in Figure S3. The measurement uncertainty was determined in terms of %CV. A heatmap of the uncertainties in measured concentrations of 150 bp dsDNA is presented in Figure 4a. The measurement uncertainty or %CV tends to decrease as the time of data acquisition and the number of nanopores increase, which is expected as the event count also increases.[38] Subsequently, the % CV values for measured %150 bp shown in the heatmap in Figure 4b also follow a similar trend. These results indicate that measurement uncertainties can still be less than 15% for the measurement of 150 bp concentration and %150 bp if the data acquisition time is reduced to 15 min for a larger number of nanopores with insignificant size variations. A CV of 15% is typically acceptable for lab-based capillary electrophoresis systems. Given its suitability for POC settings, a multiple nanopore strategy with parallel data acquisition capability can significantly reduce the turnaround time of the nanopore QC assay.

Validation of Nanopore QC Assay Using Plasma cfDNA Sample. To validate our nanopore QC assay for the quantification and qualification of cfDNA, a commercially purchased plasma sample of a healthy individual was subjected to our nanopore QC and gold standard TapeStation capillary electrophoresis (CE) assays. The time degradation study of the cfDNA was performed for 55 days after plasma separation post blood collection. The 1 mL aliquots of unused plasma were stored at −80 °C before use. The cfDNA from the 1 mL plasma aliquot was extracted in 55 μL of elution buffer on eighth, 34th, 41st, 48th, and 55th day using QIAamp circulating nucleic acid kit according to the manufacturer protocol. The extraction process is detailed in the "Materials and Methods" section. The eluate was directly subjected to TapeStation characterization. However, it was further diluted in the 4 M LiCl salt buffer by a factor of 40× for nanopore QC assay. We chose a factor of 40× dilution to allow the plasma concentrations fall in the range of 2−40 ng/mL, which will then correspond to the previously established detection range of 10−200 pM for 150 bp dsDNA. The details about the

https://doi.org/10.1021/acssensors.5c00803
ACS Sens. 2025, 10, 5674−5683

TapeStation CE assay have also been presented in the "Materials and Methods" section. The amount of cfDNA and %cfDNA for quantification and qualification were obtained from capillary electropherograms, which have been shown in Figure 5a on the left side for the respective day of cfDNA extraction post plasma separation. To calculate the concentration of cfDNA and %cfDNA from electropherograms, the area under the curve between 50 and 600 bp markings was determined and compared with the total coverage area. The known concentrations of lower and upper markers then allowed for the computation of cfDNA concentration and % cfDNA in the eluate, which were then back calculated to the original plasma concentrations, considering a 100% recovery of cfDNA from 1 mL of plasma to 55 μL of eluate. Each extracted cfDNA was also concurrently subjected to our established nanopore QC assay after dilution with 4 M LiCl measurement buffer. The nanopore QC data of each respective day of cfDNA extraction have been presented as the normalized count distributions of blockage amplitudes with their corresponding multi-Gaussian fittings in Figure 5a on the right side. A quick analysis of the data from both the TapStation CE and nanopore QC assays suggests that no HMW gDNA was detected, which is probably due to the collection of blood in streck tubes. Streck tubes are specifically designed to stabilize cfDNA and inhibit cellular degradation or hemolysis, which may cause gDNA contamination. The absence of gDNA characteristic peaks in both the TapeStation and CE assays implied that a %cfDNA was 100% and remained unaffected throughout the 7 weeks of degradation study, as shown in Figure S4. The measured concentrations of the cfDNA from each respective extraction were plotted, as shown in Figure 5b, for both TapeStation CE and nanopore QC assays. The concentration of cfDNA dropped significantly by ~71.5% from its initial concentration of 29.61 ng/mL, measured on the eighth day of extraction, to 8.44 ng/mL measured on the 34th day of extraction after plasma separation from blood. The extractions including and between the 34th and 55th days were then performed on a weekly basis to analyze the short-time trends, indicating the plasma cfDNA concentration leveling off below 10 ng/mL until the 55th day of extraction. This suggests that a plasma sample stored for longer than 1 week after separation from blood rapidly loses the quality of cfDNA in terms of the measured quantities. The quantity of cfDNA may continue to drop or level-off even after the 55th day of extraction; however, further analysis was not performed due to the lack of sample availability. Despite significantly lower input cfDNA abundance, a concentration above 2 ng/mL of cfDNA in the plasma sample has still been reported for the NGS library preparation protocols.[39] Generally, multiple extractions can be run, or the use of smaller elution buffer volumes can increase the cfDNA yield for improved coverage in sequencing workflows for healthy control samples. The concentrations of cfDNA and %cfDNA are specific to each individual, which is why the availability of a point-of-need sample QC tool can significantly add value to decision-making for sequencing library preparation, especially when the sample degradation timeline is very short. An estimated timeline for the sample-to-answer workflow of our nanopore-based sample QC is shown in Figure S5, which indicates that the cfDNA QC parameters can be determined in under 10 min after the extraction of cfDNA from plasma. A high correlation was observed for the measured cfDNA concentration between nanopore QC and TapeStation CE assays, as shown in Figure 5c. Our nanopore sensor is a label-free, electronic readout approach for sample QC with performance comparable to the conventional laboratory-based TapeStation CE assay, which suggests that it has high potential for POC implementation to complement modern-day needs of portable nanopore sequencers.

CONCLUSION

With the rapid miniaturization of sequencing technologies to enable point-of-care (POC) diagnostics for personalized healthcare, there is an urgent need for a comprehensive POC sample quality control (QC) tool. Here, we present a nanopore sensor for the assessment of cfDNA samples, amenable to point-of-need applications. By employing a 1 kb DNA marker at a known concentration, our technique precisely quantifies the varying concentrations of a 150 bp dsDNA as a representative cfDNA target in a test range of 10−200 pM in mock samples, as a quantification metric in the QC assay. Additionally, it enabled the precise measurement of %150 bp as a qualification metric of sample QC in the presence of a 10 kbp dsDNA, a representative HMW gDNA contaminant. The estimated and known values of concentration and the percentage of 150 bp dsDNA showed a high correlation of above 90%. Smaller variations in nanopore diameters (6−19 nm) minimally affected the measurements, with a CV of <15%. We have further demonstrated that the measurement uncertainty can be tuned by analyzing the cumulative data from multiple nanopores for different data acquisition times. The measurement uncertainty decreases as the number of nanopores and the data acquisition times increase. Validation studies, tracking cfDNA degradation over nearly 7 weeks using our nanopore sensor and TapeStation CE assay, showed strong correlation in concentration measurements, with significant cfDNA degradation observed after 4 weeks of plasma separation post blood collection. Given the label-free simple electronic readout capabilities, this method holds high promise as a POC amendable sample QC tool for point-of-need NGS.

MATERIALS AND METHODS

Materials and Chemicals. For nanopore fabrication, quartz capillaries with inner and outer diameters of 0.5 and 1 mm, respectively (Q100−50−7.5) were purchased from Sutter Instrument, USA. A microinjector for filling the nanopipettes (MF34G−5) was purchased from World Precision Instruments. The nanopipette holder (QSW-T10N) and 0.2 mm diameter Ag wires were purchased from Warner Instruments, USA. UltraPure DNase/RNase-Free Distilled Water (catalog number: 10977015) and the dsDNA fragments of various lengths (150 bp, 1k, and 10k bp) were purchased from Thermo Fisher. Tris-EDTA buffer solution (pH 8.0), lithium chloride (LiCl) salt, sulfuric acid (H_2SO_4), and hydrogen peroxide (H_2O_2) were purchased from Sigma-Aldrich. The QIAamp Circulating Nucleic Acid Kit (catalog number: 55114) was purchased from QIAGEN for cfDNA extraction from plasma samples. A plasma sample from a healthy control was purchased from BioCollections Worldwide, Inc. High Sensitivity D5000 (HSD5000) ScreenTape and Reagents (part numbers: 5067−5592 and 5067−5593) were purchased from Agilent Technologies.

Nanopore Fabrication. To fabricate the glass nanopores, glass capillaries were cleaned using piranha solution, which was

https://doi.org/10.1021/acssensors.5c00803
ACS Sens. 2025, 10, 5674−5683

prepared in the laboratory by mixing H_2SO_4 and H_2O_2 in a 3:1 ratio. Briefly, the capillaries immersed in piranha solution were placed on a hot plate for 30 min at 85 °C, followed by rinsing with DI water and vacuum drying at 120 °C for 20 min. The capillaries were then subjected to a two-line recipe in a laser pipette puller (P-2000, Sutter Instruments, USA) to fabricate nanopores. Line 1: "heat 750, filament 5, velocity 50, delay 140, and pull 50" and Line 2: "heat 715, filament 4, velocity 30, delay 145, and pull 215." This recipe fabricates nanopores with diameters typically around 10 nm. However, to change the nanopore diameters, we slightly adjusted the "pull" parameter in Lines 1 and 2. The nanopore diameters were estimated from open-pore conductance values obtained through *I-V* characteristics, as described in previous work.[38] The pulling parameters of the fabrication recipe are instrument specific, and the process is sensitive to the physical conditions of the environment, so the fabrication recipe can be customized to obtain the desired nanopore diameters.

Extraction and Purification of cfDNA from Plasma Samples. Various preanalytical factors may affect the total cfDNA recovery,[40] so an extensively adopted plasma processing and extraction protocol was employed. Briefly, the fresh plasma sample was obtained 2 h post blood collection from a healthy individual (with no history of HIV or cancer) following a double centrifugation procedure with a custom protocol provided by the vendor, BioCollections Worldwide, Inc., and stored immediately at −80 °C. The plasma sample was received frozen on the seventh day post plasma separation and stored at −80 °C before cfDNA extraction. The QIAamp Circulating Nucleic Acid kit has been shown to recover >90% of the total cfDNA post extraction. The extraction procedure was performed according to the manufacturer's protocol, which involved four typical steps of silica column extractions: lyse, bind, wash, and elute. One milliliter of plasma was used with an elution volume of 50 μL, and the eluted volume was then further used for Qubit, capillary electrophoresis (CE), and nanopore cfDNA QC.

Agilent TapeStation CE Assay for cfDNA Size Profiling and %cfDNA. Following the cfDNA extraction from plasma samples of healthy controls, the eluted cfDNA samples are subjected to an HSD5000 ScreenTape Assay in an Agilent TapeStation 4150 system for size profiling and % cfDNA evaluation. The HSD5000 reagents (ladder and sample buffer) are brought to room temperature for 30 min. The HSD5000 ScreenTape device is inserted into the ScreenTape nest of the 4150 TapeStation instrument. Appropriate selections of required sample positions are made in the TapeStation Controller software. Reagents and samples are vortexed and spun down before use. To prepare the ladder, 2 μL of HSD5000 sample buffer and 2 μL of the ladder are added at position A1 in a tube strip. For each sample, 2 μL of HSD5000 sample buffer and 2 μL of cfDNA sample are added at the subsequent positions in the tube strip. The tube strip is then capped, and the liquids are mixed using a vortex mixer at 2000 rpm for 1 min, followed by spinning down for 1 min. The tube strip is loaded into the 4150 TapeStation instrument by confirming the A1 position of the ladder on the tube strip holder. The cap of the tube strip is carefully removed, ensuring that all the sample volume is settled at the bottom. The instrument is run, and the TapeStation analysis software opens automatically afterward to display the results.

Data Analysis Method and Statistics. All ionic current−time (*I-t*) data were acquired at a 100 kHz sampling frequency using a patch-clamp amplifier, Axopatch 200B by Molecular Devices, an NI 6363 DAQ card, and a low-pass filter (5 kHz) in a custom LabVIEW program. Data were further analyzed using custom MATLAB and Python scripts to extract peak information and process for multi-Gaussian fittings, respectively. The Python script for obtaining counts histograms and multi-Gaussian fittings has been provided in S2. Supplementary Code. All of the measurements were repeated at least three times, unless mentioned otherwise.

■ ASSOCIATED CONTENT

Supporting Information

The Supporting Information is available free of charge at https://pubs.acs.org/doi/10.1021/acssensors.5c00803.

The current−voltage (*I-V*) characteristics of nanopores with varying sizes are presented. It further presents the count distributions and multi-Gaussian fittings of blockage amplitudes, which were used to estimate measurement uncertainties across 24 test configurations involving single to multiple nanopore readouts. Comparative data of measured %cfDNA obtained using both our nanopore-based QC assay and the conventional TapeStation CE assay from healthy plasma samples are also included. Additionally, the estimated sample-to-answer timeline for the nanopore-based QC workflow is provided. Complete Python script used to plot count distributions and perform multi-Gaussian fitting of blockage amplitudes from processed raw current−time (*I*−*t*) data is also included (PDF)

■ AUTHOR INFORMATION

Corresponding Author

Weihua Guan − *Department of Intelligent Systems Engineering, Indiana University, Bloomington, Indiana 47408, United States;* orcid.org/0000-0002-8435-9672; Email: guanw@iu.edu

Authors

Muhammad Asad Ullah Khalid − *Department of Intelligent Systems Engineering, Indiana University, Bloomington, Indiana 47408, United States;* orcid.org/0000-0001-5926-1764

Md. Ahasan Ahamed − *Department of Intelligent Systems Engineering, Indiana University, Bloomington, Indiana 47408, United States; Department of Electrical Engineering, Pennsylvania State University, University Park, Pennsylvania 16802, United States;* orcid.org/0009-0006-9962-2994

Anthony J. Politza − *Department of Biomedical Engineering, Pennsylvania State University, University Park, Pennsylvania 16802, United States;* orcid.org/0009-0005-8670-2357

Complete contact information is available at: https://pubs.acs.org/10.1021/acssensors.5c00803

Notes

A preprint of this article, deposited in bioRxiv, can be found at 10.1101/2025.03.17.643726.

The authors declare no competing financial interest.

■ ACKNOWLEDGMENTS

This work was partially supported by the National Science Foundation (2319913, 2045169), the National Institutes of Health (R33AI147419), and the USDA (NIFA 2022-11225).

Any opinions, findings, conclusions, or recommendations expressed in this work are those of the authors and do not necessarily reflect the views of the National Science Foundation, the National Institutes of Health, or the USDA.

REFERENCES

(1) Bertoli-Avella, A. M.; Beetz, C.; Ameziane, N.; Rocha, M. E.; Guatibonza, P.; Pereira, C.; Calvo, M.; Herrera-Ordonez, N.; Segura-Castel, M.; Diego-Alvarez, D.; Zawada, M.; Kandaswamy, K. K.; Werber, M.; Paknia, O.; Zielske, S.; Ugrinovski, D.; Warnack, G.; Kampe, K.; Iuraşcu, M.-I.; Cozma, C.; Vogel, F.; Alhashem, A.; Hertecant, J.; Al-Shamsi, A. M.; Alswaid, A. F.; Eyaid, W.; Al Mutairi, F.; Alfares, A.; Albalwi, M. A.; Alfadhel, M.; Al-Sannaa, N. A.; Reardon, W.; Alanay, Y.; Rolfs, A.; Bauer, P. Successful Application of Genome Sequencing in a Diagnostic Setting: 1007 Index Cases from a Clinically Heterogeneous Cohort. *Eur. J. Hum. Genet.* **2021**, *29* (1), 141−153.

(2) Oehler, J. B.; Wright, H.; Stark, Z.; Mallett, A. J.; Schmitz, U. The Application of Long-Read Sequencing in Clinical Settings. *Hum. Genomics* **2023**, *17* (1), 73.

(3) Zhong, Y.; Xu, F.; Wu, J.; Schubert, J.; Li, M. M. Application of Next Generation Sequencing in Laboratory Medicine. *Ann. Lab. Med.* **2021**, *41* (1), 25−43.

(4) Dewey, F. E.; Pan, S.; Wheeler, M. T.; Quake, S. R.; Ashley, E. A. DNA Sequencing: Clinical Applications of New DNA Sequencing Technologies. *Circulation* **2012**, *125* (7), 931−944.

(5) Crossley, B. M.; Bai, J.; Glaser, A.; Maes, R.; Porter, E.; Killian, M. L.; Clement, T.; Toohey-Kurth, K. Guidelines for Sanger Sequencing and Molecular Assay Monitoring. *J. Vet. Diagn. Invest.* **2020**, *32* (6), 767−775.

(6) Kumar, K. R.; Cowley, M. J.; Davis, R. L. Next-Generation Sequencing and Emerging Technologies*. *Semin. Thromb. Hemostasis* **2024**, *50* (7), 1026−1038.

(7) Slatko, B. E.; Gardner, A. F.; Ausubel, F. M. Overview of Next-Generation Sequencing Technologies. *Curr. Protoc. Mol. Biol.* **2018**, *122* (1), No. e59.

(8) Metzker, M. L. Sequencing Technologies—the next Generation. *Nat. Rev. Genet.* **2010**, *11* (1), 31−46.

(9) Rhoads, A.; Au, K. F. PacBio Sequencing and Its Applications. *Genomics, Proteomics Bioinf.* **2015**, *13* (5), 278−289.

(10) Hussen, B. M.; Abdullah, S. T.; Salihi, A.; Sabir, D. K.; Sidiq, K. R.; Rasul, M. F.; Hidayat, H. J.; Ghafouri-Fard, S.; Taheri, M.; Jamali, E. The Emerging Roles of NGS in Clinical Oncology and Personalized Medicine. *Pathol., Res. Pract.* **2022**, *230*, 153760.

(11) Andrade, M. D. S.; Campos, F. S.; Campos, A. A. S.; Abreu, F. V. S.; Melo, F. L.; Sevá, A. D. P.; Cardoso, J. D. C.; Dos Santos, E.; Born, L. C.; Silva, C. M. D. D.; Müller, N. F. D.; Oliveira, C. H. D.; Silva, A. J. J. D.; Simonini-Teixeira, D.; Bernal-Valle, S.; Mares-Guia, M. A. M. M.; Albuquerque, G. R.; Romano, A. P. M.; Franco, A. C.; Ribeiro, B. M.; Roehe, P. M.; Almeida, M. A. B. D. Real-Time Genomic Surveillance during the 2021 Re-Emergence of the Yellow Fever Virus in Rio Grande Do Sul State, Brazil. *Viruses* **2021**, *13* (10), 1976.

(12) Inzaule, S. C.; Tessema, S. K.; Kebede, Y.; Ogwell Ouma, A. E.; Nkengasong, J. N. Genomic-Informed Pathogen Surveillance in Africa: Opportunities and Challenges. *Lancet Infect. Dis.* **2021**, *21* (9), No. e281−e289.

(13) Fagerlund, A.; Idland, L.; Heir, E.; Møretrø, T.; Aspholm, M.; Lindbäck, T.; Langsrud, S. Whole-Genome Sequencing Analysis of Listeria Monocytogenes from Rural, Urban, and Farm Environments in Norway: Genetic Diversity, Persistence, and Relation to Clinical and Food Isolates. *Appl. Environ. Microbiol.* **2022**, *88* (6), No. e02136−21.

(14) Marcozzi, A.; Jager, M.; Elferink, M.; Straver, R.; Van Ginkel, J. H.; Peltenburg, B.; Chen, L.-T.; Renkens, I.; Van Kuik, J.; Terhaard, C.; De Bree, R.; Devriese, L. A.; Willems, S. M.; Kloosterman, W. P.; De Ridder, J. Accurate Detection of Circulating Tumor DNA Using Nanopore Consensus Sequencing. *Npj Genomic Med.* **2021**, *6* (1), 106.

(15) Van Der Pol, Y.; Tantyo, N. A.; Evander, N.; Hentschel, A. E.; Wever, B. M.; Ramaker, J.; Bootsma, S.; Fransen, M. F.; Lenos, K. J.; Vermeulen, L.; Schneiders, F. L.; Bahce, I.; Nieuwenhuijzen, J. A.; Steenbergen, R. D.; Pegtel, D. M.; Moldovan, N.; Mouliere, F. Real-time Analysis of the Cancer Genome and Fragmentome from Plasma and Urine Cell-free DNA Using Nanopore Sequencing. *EMBO Mol. Med.* **2023**, *15* (12), No. e17282.

(16) Sampathi, S.; Chernyavskaya, Y.; Haney, M. G.; Moore, L. H.; Snyder, I. A.; Cox, A. H.; Fuller, B. L.; Taylor, T. J.; Badgett, T. C.; Blackburn, J. S. Nanopore Sequencing Methods Detect Cell-Free DNA Associated with MRD and CNS Infiltration in Pediatric Acute Lymphoblastic Leukemia. *bioRixv*. **2021**.

(17) King, J.; Harder, T.; Beer, M.; Pohlmann, A. Rapid Multiplex MinION Nanopore Sequencing Workflow for Influenza A Viruses. *BMC Infect. Dis.* **2020**, *20* (1), 648.

(18) Johansson, G.; Andersson, D.; Filges, S.; Li, J.; Muth, A.; Godfrey, T. E.; Ståhlberg, A. Considerations and Quality Controls When Analyzing Cell-Free Tumor DNA. *Biomol. Detect. Quantif.* **2019**, *17*, 100078.

(19) Hess, J. F.; Kohl, T. A.; Kotrová, M.; Rönsch, K.; Paprotka, T.; Mohr, V.; Hutzenlaub, T.; Brüggemann, M.; Zengerle, R.; Niemann, S.; Paust, N. Library Preparation for next Generation Sequencing: A Review of Automation Strategies. *Biotechnol. Adv.* **2020**, *41*, 107537.

(20) Nesic, M.; Bødker, J. S.; Terp, S. K.; Dybkær, K. Optimization of Preanalytical Variables for cfDNA Processing and Detection of ctDNA in Archival Plasma Samples. *Biomed Res. Int.* **2021**, *2021*, 1−9.

(21) Maass, K. K.; Schad, P. S.; Finster, A. M. E.; Puranachot, P.; Rosing, F.; Wedig, T.; Schwarz, N.; Stumpf, N.; Pfister, S. M.; Pajtler, K. W. From Sampling to Sequencing: A Liquid Biopsy Pre-Analytic Workflow to Maximize Multi-Layer Genomic Information from a Single Tube. *Cancers* **2021**, *13* (12), 3002.

(22) Bohers, E.; Viailly, P.-J.; Jardin, F. cfDNA Sequencing: Technological Approaches and Bioinformatic Issues. *Pharmaceuticals* **2021**, *14* (6), 596.

(23) Pös, Z.; Pös, O.; Styk, J.; Mocova, A.; Strieskova, L.; Budis, J.; Kadasi, L.; Radvanszky, J.; Szemes, T. Technical and Methodological Aspects of Cell-Free Nucleic Acids Analyzes. *IJMS* **2020**, *21* (22), 8634.

(24) Bronkhorst, A. J.; Ungerer, V.; Holdenrieder, S. Comparison of Methods for the Quantification of Cell-Free DNA Isolated from Cell Culture Supernatant. *Tumour Biol.* **2019**, *41* (8), 101042831986636.

(25) Ponti, G.; Maccaferri, M.; Manfredini, M.; Kaleci, S.; Mandrioli, M.; Pellacani, G.; Ozben, T.; Depenni, R.; Bianchi, G.; Pirola, G. M.; Tomasi, A. The Value of Fluorimetry (Qubit) and Spectrophotometry (NanoDrop) in the Quantification of Cell-Free DNA (cfDNA) in Malignant Melanoma and Prostate Cancer Patients. *Clin. Chim. Acta* **2018**, *479*, 14−19.

(26) García-Alegría, A. M.; Anduro-Corona, I.; Pérez-Martínez, C. J.; Guadalupe corella-Madueño, M. A.; Rascón-Durán, M. L.; Astiazaran-Garcia, H. Quantification of DNA through the NanoDrop Spectrophotometer: Methodological Validation Using Standard Reference Material and Sprague Dawley Rat and Human DNA. *Int. J. Anal. Chem.* **2020**, *2020*, 1−9.

(27) Nakayama, Y.; Yamaguchi, H.; Einaga, N.; Esumi, M. Pitfalls of DNA Quantification Using DNA-Binding Fluorescent Dyes and Suggested Solutions. *PLoS One* **2016**, *11* (3), No. e0150528.

(28) Ungerer, V.; Bronkhorst, A. J.; Uhlig, C.; Holdenrieder, S. Cell-Free DNA Fragmentation Patterns in a Cancer Cell Line. *Diagnostics* **2022**, *12* (8), 1896.

(29) Gordon, M. J.; Huang, X.; Pentoney, S. L.; Zare, R. N. Capillary Electrophoresis. *Science* **1988**, *242* (4876), 224−228.

(30) Saelee, S. L.; Lovejoy, A. F.; Hinzmann, B.; Mayol, K.; Huynh, S.; Harrell, A.; Lefkowitz, J.; Deodhar, N.; Garcia-Montoya, G.; Yaung, S. J.; Klass, D. M. Quantitative PCR−Based Method to Assess Cell-Free DNA Quality, Adjust Input Mass, and Improve Next-Generation Sequencing Assay Performance. *J. Mol. Diagn.* **2022**, *24* (6), 566−575.

https://doi.org/10.1021/acssensors.5c00803
ACS Sens. 2025, 10, 5674−5683

(31) Terp, S. K.; Pedersen, I. S.; Stoico, M. P. Extraction of Cell-Free DNA. *J. Mol. Diagn.* **2024**, *26* (4), 310−319.
(32) Sorber, L.; Zwaenepoel, K.; Deschoolmeester, V.; Roeyen, G.; Lardon, F.; Rolfo, C.; Pauwels, P. A Comparison of Cell-Free DNA Isolation Kits. *J. Mol. Diagn.* **2017**, *19* (1), 162−168.
(33) Li, H.; Li, Y.; Gui, C.; Chen, D.; Chen, L.; Luo, L.; Huang, G.; Yuan, Y.; He, R.; Xia, F.; Wang, J. Bare Glassy Nanopore for Length-Resolution Reading of PCR Amplicons from Various Pathogenic Bacteria and Viruses. *Talanta* **2023**, *256*, 124275.
(34) Charron, M.; Briggs, K.; King, S.; Waugh, M.; Tabard-Cossa, V. Precise DNA Concentration Measurements with Nanopores by Controlled Counting. *Anal. Chem.* **2019**, *91* (19), 12228−12237.
(35) Israelachvili, J. N. *Intermolecular and Surface Forces*, 3rd ed.; Academic press: Burlington, Mass., 2011.
(36) Chen, K.; Bell, N. A. W.; Kong, J.; Tian, Y.; Keyser, U. F. Direction- and Salt-Dependent Ionic Current Signatures for DNA Sensing with Asymmetric Nanopores. *Biophys. J.* **2017**, *112* (4), 674−682.
(37) Nouri, R.; Tang, Z.; Guan, W. Quantitative Analysis of Factors Affecting the Event Rate in Glass Nanopore Sensors. *ACS Sens.* **2019**, *4* (11), 3007−3013.
(38) Nouri, R.; Tang, Z. F.; Guan, W. H. Calibration-Free Nanopore Digital Counting of Single Molecules. *Anal. Chem.* **2019**, *91* (17), 11178−11184.
(39) Alborelli, I.; Generali, D.; Jermann, P.; Cappelletti, M. R.; Ferrero, G.; Scaggiante, B.; Bortul, M.; Zanconati, F.; Nicolet, S.; Haegele, J.; Bubendorf, L.; Aceto, N.; Scaltriti, M.; Mucci, G.; Quagliata, L.; Novelli, G. Cell-Free DNA Analysis in Healthy Individuals by next-Generation Sequencing: A Proof of Concept and Technical Validation Study. *Cell Death Dis.* **2019**, *10* (7), 534.
(40) Page, K.; Guttery, D. S.; Zahra, N.; Primrose, L.; Elshaw, S. R.; Pringle, J. H.; Blighe, K.; Marchese, S. D.; Hills, A.; Woodley, L.; Stebbing, J.; Coombes, R. C.; Shaw, J. A. Influence of Plasma Processing on Recovery and Analysis of Circulating Nucleic Acids. *PLoS One* **2013**, *8* (10), No. e77963.

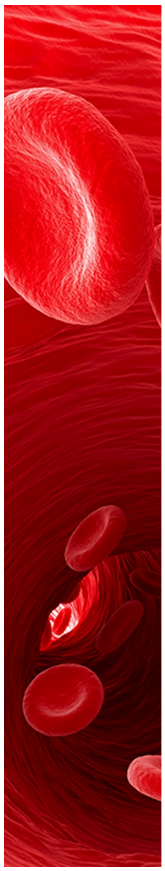
CAS BIOFINDER DISCOVERY PLATFORM™
CAS BIOFINDER HELPS YOU FIND YOUR NEXT BREAKTHROUGH FASTER
Navigate pathways, targets, and diseases with precision
Explore CAS BioFinder
CAS
A division of the American Chemical Society

https://doi.org/10.1021/acssensors.5c00803
ACS Sens. 2025, 10, 5674−5683